

Boundary effect of a partition in a quantum well

Tamás Fülöp,^{a,1,*}, Izumi Tsutsui^b

^a*Nuclear Physics Institute, Academy of Sciences, 25068 Řež near Prague, Czech Republic*

^b*Institute of Particle and Nuclear Studies, High Energy Accelerator Research Organization (KEK), Tsukuba 305-0801, Japan*

Abstract

We consider a system of identical particles, bosons or fermions, at finite temperatures confined in a one dimensional quantum well which has a partition in the center. Assuming nontrivial boundary conditions (Dirichlet on one side and Neumann on the other) for the partition, we study by numerical and analytic means the net pressure that emerges on the partition due to the difference in the energy levels between the two half wells separated by the partition. The quantum pressure has a single minimum in the medium temperature regime and exhibits a number of intriguing features, such as the scaling (square root) law for the diverging high temperature asymptotics and the distinctive dependences on the particle numbers characterizing the statistics of the particles. Our analytical approximations yield results which can account for these features and fit the numerical curves of the pressure reasonably well.

Key words: quantum mechanics, infinite potential well, boundary conditions, quantum statistical mechanics, Bose-Einstein, Fermi-Dirac, pressure, force

PACS: 03.65.-w, 02.30.Mv, 02.30.Tb, 02.60.-x, 02.60.Lj, 05.30.-d, 05.30.Jp, 05.30.Fk

^{*} Corresponding author.

Email addresses: tamas.fulop@gmail.com (Tamás Fülöp,), izumi.tsutsui@kek.jp (Izumi Tsutsui).

¹ Postdoctoral fellow at the Doppler Institute for Mathematical Physics and Applied Mathematics, Prague, Czech Republic

1 Introduction

Quantum singularity is a point defect in an otherwise ‘regular’ system treated in quantum mechanics. Despite the simple setting, such a system exhibits various features which are intriguing both mathematically and physically. On mathematical sides, it permits rich structures admitted under the general class of self-adjoint Hamiltonians describing the system. The mathematically allowed class is rather large, but when the system is linear (*i.e.*, one dimensional), it is concisely characterized by the unitary group $U(2)$ (see, *e.g.*, [1–3]) which includes, among others, the familiar singular interactions realized by the Dirac delta potentials with arbitrary strengths. On physical sides, one the other hand, the quantum singularity admits interesting phenomena such as duality, supersymmetry, anholonomy (Berry phase) and spontaneous symmetry breaking [4–6] (see also [7]). An application for a qubit device, which might become realizable by future development of nanotechnology, has also been suggested [8].

All the studies on quantum singularity mentioned above have assumed one-particle systems at zero temperature, but since actual realizations of the systems would involve many particles acting under finite temperatures, it should be inevitable to take into account the statistical aspects of the particles. The aim of this paper is to present a case study of such statistical aspects by analyzing a system which is both simple and familiar – a quantum well. Specifically, we consider particles in a quantum well with a partition placed in the center. The partition is made by an infinitely thin wall which forms a single point defect inside the well. The partition separates the well into two half wells, each of which is supposed to contain N identical particles. For the statistics of the particles, we consider separately the two cases, the Bose-Einstein and the Fermi-Dirac statistics, and the entire well is put under various temperatures, ranging from zero to infinity.

To characterize the partition in a simplest nontrivial term, we assume that the partition enforces the Dirichlet condition on the left and the Neumann on the right (see Fig. 1), which is perhaps a simplest nontrivial combination permitted quantum mechanically. We focus on the pressure, or statistical quantum force, acting on the partition, which arises from the discordance in energy levels between the two half wells [9]. We shall be content to work in the one dimensional setup, but the extension to multi-dimensions will be done analogously by considering the class of singularities pertinent to the dimensions.

The temperature behavior of the net quantum force — the difference between the pressures from the left and the right of the partition — exhibits a number of interesting and unexpected features. For instance, the force curve as a function of temperature starts off with a finite value at the zero temperature and reaches

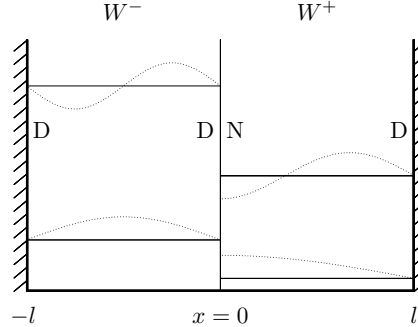


Fig. 1. Quantum well with a partition at the center. Under the Dirichlet ($\psi = 0$) and Neumann ($\psi' = 0$) boundary conditions on the left and the right of the partition (while we choose the Dirichlet for the two ends of the well), the eigenstates (the lowest two are shown in both half wells W^\pm) have different energy levels. When the same number N of particles are introduced in each of the half wells, these level differences lead to a net force on the partition which exhibits interesting temperature behaviors.

a single minimal point at a finite temperature before diverging in the high temperature limit according to a certain scaling law, *i.e.*, the square root of the temperature. This overall temperature behavior can be observed for both the bosonic and the fermionic cases, but in the latter case the curve in the low temperature regime shows an additional little twist which is absent in the former. Another feature worth mentioning is the distinct characteristics of the dependence on the number of particles; *e.g.*, both the zero temperature value and the minimal force are of the order of N for bosons while they are of the order of N^2 for fermions.

Our analysis on the quantum force is carried out both numerically and analytically. Some of the initial results have been reported earlier [10,11], and here we shall present the full detail of our complete analysis, including the analytical approximations performed with assistance of numerical solutions of some transcendental equation. We shall see that our goal to find analytic formulae that can account for the pure numerical results as well as the statistical feature of the particle number dependence mentioned above is achieved reasonably well. Our outcomes illustrate how quantum singularity, realized by a partition in the present model of a quantum well, can give rise to physically measurable effects in a plain form such as pressure.

This paper is organized as follows. In sect. 2 we provide the basic account of our model as well as the overall features of the quantum force obtained by numerical computations for all temperature regions. In sect. 3, we present the analysis for the high temperature limit where the force exhibits the common scaling behavior for the two types of particle statistics. Sect. 4 is devoted to the analysis of the medium temperature regime where the force curve has a min-

imal point. Our argument for the analytic approximation is given for bosons and fermions, separately, since the statistical difference becomes important in this regime. Similarly, sect. 5 is devoted to the analysis of the low temperature regime where the force possesses the characteristics of the N -dependence and further develops the twist in the fermionic case. In sect. 6 we briefly mention two physical quantities, the shift of partition and the transfer of particles between the two half wells, as alternatives which may be more directly observed than the quantum force. Finally, we present our conclusion and discussions in sect. 7. Appendix A gives the outline of our numerical computation, and Appendix B contains the technical detail of our approximation employed in sect. 4.

2 Quantum force on a partition and its temperature behaviors

Before we present our full analysis of the quantum force, we provide the basic account of the system for which we discuss the boundary effect for various temperature regions.

The system we consider is a one-dimensional quantum well W possessing a partition wall at the center, given by the interval $[-l, l]$ with the partition at $x = 0$. To define the system in quantum mechanics, we need to specify the boundary conditions for the wave function $\psi(x)$ imposed both at the two ends of the well $x = \pm l$ and at the partition on its left and right sides $x = \pm 0$. In quantum mechanics, allowed boundary conditions are those which respect the probability conservation requirement. If we assume that the partition is impenetrable, *i.e.*, the particles cannot penetrate the partition, then the most general form of the is given by

$$\psi(\pm l) + L_{\pm l} \psi'(\pm l) = 0, \quad \psi(\pm 0) + L_{\pm 0} \psi'(\pm 0) = 0, \quad (1)$$

where $L_{\pm l}$, $L_{\pm 0}$ are arbitrary real constants including infinity. For instance, $L_{+0} = 0$ in (1) implies the Dirichlet condition $\psi(+0) = 0$ whereas $L_{+0} = \infty$ implies the Neumann condition $\psi'(+0) = 0$ at $x = +0$. Similar choices of boundary conditions should be made at the other three points, $x = \pm l$ and $x = -0$ by specifying the constants $L_{\pm l}$ and L_{-0} [12].

In this paper, to realize a nontrivial partition in the simplest setting, we adopt the set of boundary conditions provided by $L_{\pm l} = 0$, $L_{+0} = \infty$ and $L_{-0} = 0$, that is, the Neumann boundary condition at the right side $x = +0$ and the Dirichlet at the left side $x = -0$ of the partition as well as at the both ends $x = \pm l$ of the wall:

$$\psi(-l) = 0, \quad \psi(-0) = 0, \quad \psi'(+0) = 0, \quad \psi(l) = 0. \quad (2)$$

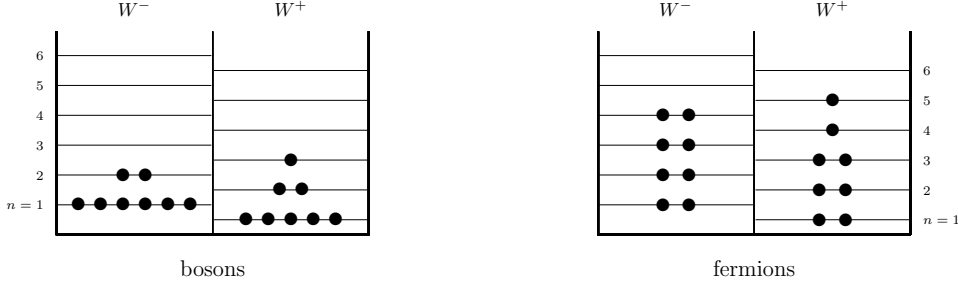


Fig. 2. Illustration of the distribution of particles over the levels in the two half wells at a low temperature. In the fermionic example $s = 1/2$ is assumed. The gap of the levels and the difference in the populations in the two wells induce a non-vanishing force on the partition, which is dependent on the temperature as well as the particle statistics.

The quantum well W is then split into two half, physically distinct, wells W^+ and W^- by the partition. In the two half wells W^\pm with the boundary conditions (2), the free Hamiltonian

$$H = -\frac{\hbar^2}{2m} \frac{d^2}{dx^2} \quad (3)$$

admits energy levels

$$E_n = e_n \mathcal{E}, \quad \mathcal{E} = \frac{\hbar^2}{2m} \left(\frac{\pi}{l}\right)^2, \quad n = 1, 2, 3, \dots, \quad (4)$$

which are distinct for the two half wells (see Fig. 1),

$$e_n = \begin{cases} \left(n - \frac{1}{2}\right)^2 & \text{for } W^+, \\ n^2 & \text{for } W^-. \end{cases} \quad (5)$$

It is then expected that the level gap between the two half wells W^\pm gives rise to noticeable physical effects, and one obvious example will be the force (or pressure) acting on the partition due to the difference of the pressures exerted by particles inside the two half wells. To extract the pure boundary effect, we put an identical number of particles in each of the half wells, and thereby study the temperature dependence of the net force emerging on the partition. We do this for the two cases of particle statistics, bosons and fermions, which possess different features because of the different statistical distributions over the energy levels (see Fig. 2).

To be more explicit, let N denote the number of the identical particles in both of the two half wells W^\pm in each of the $2s + 1$ spin degrees of freedom, where

s is the spin of the particles. At temperature T , the particles distribute over the levels according to the population number (per spin degree of freedom)

$$N_n = \frac{1}{e^{\alpha+be_n} - \eta}, \quad (6)$$

where we have introduced the statistical index,

$$\eta = (-1)^{2s} = \begin{cases} 1 & \text{for bosons} \\ -1 & \text{for fermions} \end{cases} \quad (7)$$

and the shorthand

$$b = \frac{\mathcal{E}}{kT} \quad (8)$$

with k being the Boltzmann constant and \mathcal{E} given in (4). The temperature-dependent quantity α is determined by the total particle number constraint,

$$N = \sum_n N_n. \quad (9)$$

The force acting on the partition from one side is then given by

$$F = -(2s+1) \sum_n N_n \frac{\partial E_n}{\partial l} = (2s+1) \frac{2\mathcal{E}}{l} \sum_n N_n e_n, \quad (10)$$

which is simplified as

$$f = \sum_n N_n e_n, \quad (11)$$

in terms of the reduced (dimensionless) force defined by

$$f = \frac{1}{2s+1} \frac{l}{2\mathcal{E}} F. \quad (12)$$

Denoting by f^\pm the forces on the partition in the half wells W^\pm , we have the net force on the partition (from the left to the right),

$$\Delta f = f^- - f^+. \quad (13)$$

Throughout the paper we use the superscripts \pm to refer to quantities pertaining to the half wells W^\pm , respectively, and also use Δ to refer to the

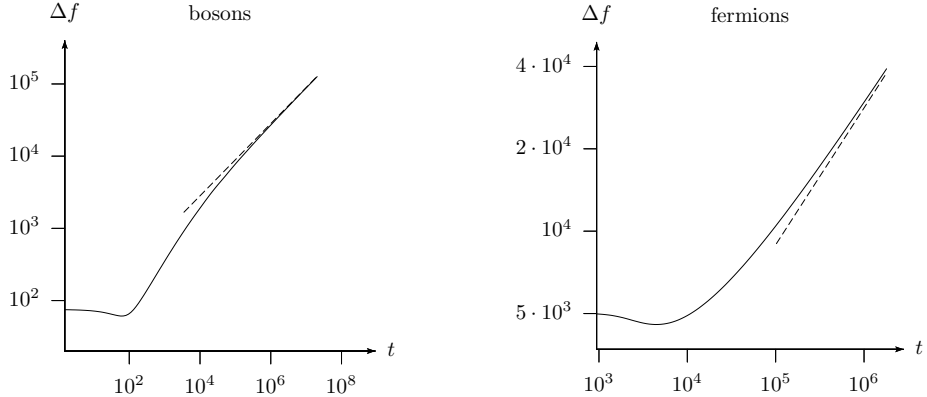


Fig. 3. Double logarithmic plot of the net force Δf as the function of the temperature variable t , for bosons (left) and fermions (right), at $N = 100$, obtained by a numerical computation (solid line). Their common high-temperature asymptotics (23) is also displayed (dashed line).

difference between the two quantities such as (13). However, we will often omit these superscripts for brevity as long as the distinction is unnecessary in the argument.

Our aim will be to determine the net force Δf in (13) as a function of the temperature. For our later convenience, we introduce the reduced temperature t by

$$t = \frac{1}{b} = \frac{k}{\mathcal{E}} T. \quad (14)$$

Numerical evaluations of Δf in terms of t can be achieved readily for finite N , and the outcome for $N = 100$ and $s = 0$ is shown in Fig. 3 for the whole range of t . We observe immediately there that (i) the net force has a finite zero temperature limit, (ii) it exhibits a power law (as it approaches the dotted straight line) in the high temperature limit, and (iii) it has a single minimum in between. These overall features are common both in the bosonic and fermionic cases, and can be seen for other values of N different from $N = 100$ as well. The basic difference between the bosonic and fermionic cases lies in the fact that the strength of the force is of the order of N for bosons while it is of the order of N^2 for fermions. Interestingly, the same difference in the N dependence can also be seen for the temperature value of the minimum force. In most part of our discussions, the numerical results will be presented for $N = 100$ particles in each spin degree of freedom (which is already a realistic population number in nanoscale quantum experiments [13]), but the conclusion remains the same for larger N .

Analytical evaluations of the force, in contrast, are not readily obtained, since the required sums in (12) cannot be performed exactly, and an analytical

solution for α which has to be determined is also difficult to find. We are thus forced to apply some approximations, but the standard approach of approximating the sum with an integral turns out to be insufficient to get the accuracy needed in the present situation, leaving us to work out novel methods for the present problem. For instance, the Fermi-Dirac integral, which is often used to approximate the sum and is related to the Lerch transcendent, can be expressed via an asymptotic series [14], but the truncations of the series do not provide enough precision to recover the force difference obtained numerically. As we shall see soon, our approximations developed in this paper and performed partly with the help of numerical solutions for transcendental equations provide formulae which fit the numerical results reasonably well. In particular, the three salient features (i), (ii) and (iii) mentioned above will be seen to be all reproduced properly by our analytic methods.

3 High temperature regime

As we have seen from the numerical results mentioned in Fig. 3, in the high-temperature limit the force Δf exhibits a certain scaling behavior which is common to both the bosonic and fermionic cases. We first show that this scaling behavior can be explained analytically based on a rather simple argument which is completely analogous in the two cases.

To study the high-temperature regime, we first note that the population number N_1 decreases for increasing temperature (see (6) for $n = 1$) and, accordingly, we expect α to increase to higher positive values for large t (or small b). It follows that the factor

$$q := e^{-\alpha} \tag{15}$$

will be extremely small in the high-temperature regime (recall that α is a function of t), and this leads us to expand N_n in q as

$$N_n = \frac{qe^{-be_n}}{1 - \eta q e^{-be_n}} = \eta^{-1} \sum_{k=1}^{\infty} (\eta q)^k e^{-kbe_n}, \tag{16}$$

with η given in (7), which is valid for any positive α . Thus we find

$$\eta N = \eta \sum_{n=1}^{\infty} N_n = \sum_{k=1}^{\infty} (\eta q)^k \sum_{n=1}^{\infty} e^{-kbe_n} = \sum_{k=1}^{\infty} (\eta q)^k \left[-\frac{\sigma}{2} + \frac{1}{2} \sum_{n=-\infty}^{\infty} e^{-kbe_n} \right], \tag{17}$$

where we have introduced the constants $\sigma^+ = 0$, $\sigma^- = 1$ corresponding to

the half wells W^\pm , and extended the meaning of the notation e_n [see (5)] to negative n as well. Applying the Poisson summation formula

$$\sum_{n=-\infty}^{\infty} y(n) = \sum_{m=-\infty}^{\infty} \int_{-\infty}^{\infty} du y(u) e^{2\pi i m u}, \quad (18)$$

we obtain

$$\eta N = \sum_{k=1}^{\infty} (\eta q)^k \left[-\frac{\sigma}{2} + \sqrt{\frac{\pi}{4kb}} \sum_{m=-\infty}^{\infty} (2\sigma - 1)^m e^{-\frac{\pi^2}{kb} m^2} \right], \quad (19)$$

where we note that the factor $2\sigma^\pm - 1$ is simply ∓ 1 . Similarly, for the force f , one can find

$$\begin{aligned} f &= \sum_{n=1}^{\infty} N_n e_n \\ &= \eta^{-1} \sum_{k=1}^{\infty} (\eta q)^k \sqrt{\frac{\pi}{16k^3 b^3}} \sum_{m=-\infty}^{\infty} (2\sigma - 1)^m \left(1 - \frac{2\pi^2}{kb} m^2 \right) e^{-\frac{\pi^2}{kb} m^2}. \end{aligned} \quad (20)$$

In the high-temperature asymptotic limit $b \rightarrow 0$, we have $q \rightarrow 0$ and hence it suffices to consider only the first few terms in the sums over k [both in (19) and (20)], and within each term to keep only the $m = 0$ term in the sums over m (the $m \neq 0$ terms being exponentially suppressed). Now, the leading $k = 1$ term in (19) gives

$$q = 2N \left(\frac{b}{\pi} \right)^{1/2} + \mathcal{O}(b). \quad (21)$$

This result shows that, for high temperatures, α tends to infinity logarithmically. Since this leading behavior of q is independent of σ , inserting it into (20) gives that the leading $\mathcal{O}(b^{-1})$ term of f (coming from $k = 1, m = 0$) is also σ -independent. Hence, the contribution coming from this term will cancel out between the two forces f^+ and f^- in the net force (13).

The first nonvanishing contribution for the net force comes from the first subleading term in q . Incorporating the $k = 2$ term as well for q , we find

$$q = 2N \left(\frac{b}{\pi} \right)^{1/2} + 2N \left[\sigma - \eta \sqrt{2} N \right] \frac{b}{\pi} + \mathcal{O}(b^{3/2}). \quad (22)$$

Plugging this into (20) and calculating the net force (13) we obtain

$$\Delta f = \frac{N}{2} \left(\frac{t}{\pi} \right)^{1/2} + \mathcal{O}(t^0), \quad (23)$$

which shows that the net force diverges asymptotically as $t \rightarrow \infty$ according to the square root of t , and that it is proportional to the particle number N . Note that these are true both for the bosonic case and the fermionic case. These results explain the high temperature asymptotic behaviors observed by the numerical analysis in Fig.3.

By incorporating higher orders, the approximation may be improved easily. For example, by taking account of the next order, one finds

$$\Delta f = \frac{N}{2} \left(\frac{t}{\pi} \right)^{1/2} - \frac{N}{\pi} \left[(\sqrt{2} - 1)\eta N - \frac{1}{2} \right] + \mathcal{O}(t^{-1/2}). \quad (24)$$

This improvement, however, is not sufficient for describing the behavior of the quantum force in lower (medium) temperature regimes where the force takes its minimum.

4 Medium temperature regime

Apart from the strength of the force, the overall shape of the force curve – for all temperature regimes – agrees for bosons and fermions. Indeed, for both of the statistical cases, the force starts with a finite value at $t = 0$ followed by a plateau and then by a steady decrease for larger t , and it exhibits even quantitatively the same high-temperature behavior for $t \rightarrow \infty$ as discussed in section 3. Moreover, the force admits only one minimum between the two limiting domains (see Fig. 3) for the two cases. A closer inspection of the curve reveals, however, that in the medium temperature regime the two cases differ in scalings with respect to the particle number N . Explicitly, our numerical results (see Fig. 4) show that, for $N \gg 1$, the value of the minimum Δf_{\min} and the temperature t_{\min} where the minimum occurs are both proportional to N for bosons, while they are proportional to N^2 for fermions. We now give an account of these distinctive features characterizing the statistics of the particles by analytic means.

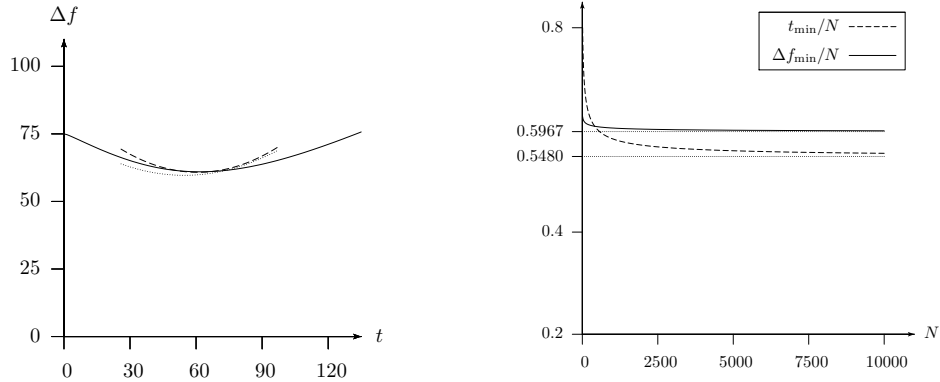


Fig. 4. (Left) The minimum of the force curve, for bosons, at $N = 100$. Solid line: numerical computation; dashed line: the approximation (40); dotted line: the approximation (44). (Right) Numerically observed scaling behaviors of the minimum force Δf_{\min} and the temperature t_{\min} at which the minimum occurs. The limiting values determined in (35) are also displayed.

4.1 Bosons

To analyze the regime of temperatures including the minimum t_{\min} for the bosonic case, we note that interpolating between the slow logarithmic increase of α for high temperature and the low-temperature behavior (64) of α (which will be derived in sect. 5) suggests the existence of a temperature regime fulfilling

$$b \ll 1, \quad |\alpha| \ll 1. \quad (25)$$

This is the ‘medium temperature regime’ we wish to consider here. Our procedure to derive the force difference is based on an approximation for α fulfilling these conditions in (25), and we confirm the consistency of our argument by examining the validity of the conditions later.

To proceed, we first solve the constraint (9) for α by approximating the sum as

$$N = \sum_{n=1}^{\infty} \frac{1}{e^{\alpha+be_n} - 1} \approx \sum_{n=1}^{\infty} \frac{1}{\alpha + be_n}. \quad (26)$$

This approximation must be good at least for the lower levels — the ones that provide the dominant contribution in the sum (note that N_n falls rapidly with n). Let us write this in the rearranged form

$$\frac{N}{t} \approx \sum_{n=1}^{\infty} \frac{1}{t\alpha + e_n}. \quad (27)$$

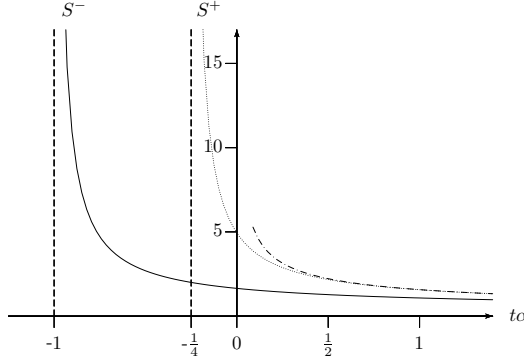


Fig. 5. The functions S^+ (dotted line) and S^- (solid line) as defined in (28). They are smooth at zero, and diverge at $-e_1^+$ resp. $-e_1^-$, where the $n = 1$ term in (28) diverges. The dashed line depicts the approximation for S^+ around 1 that is based on (38).

If one solves this in favor of $t\alpha$, then the solution will be a function of $\frac{t}{N}$. Using the standard expansion formula (see, *e.g.*, page 42 of [15]), we find that the summation in (27) is evaluated as

$$S(t\alpha) := \sum_{n=1}^{\infty} \frac{1}{t\alpha + (n - \tau)^2} = \begin{cases} \frac{\pi \tanh \pi \sqrt{t\alpha}}{2\sqrt{t\alpha}} & \text{for } W^+, \\ \frac{\pi \sqrt{t\alpha} \coth \pi \sqrt{t\alpha} - 1}{2t\alpha} & \text{for } W^-, \end{cases} \quad (28)$$

where we have used

$$\tau := \begin{cases} \frac{1}{2} & \text{for } W^+, \\ 0 & \text{for } W^-. \end{cases} \quad (29)$$

Both formulas in (28) are valid for negative α as well, and are a smooth function of $t\alpha$ at zero, see Fig. 5. Then, for a given t , or given t/N , we should solve the transcendental equations

$$S^{\pm}(t\alpha^{\pm}) = \frac{N}{t} \quad (30)$$

to obtain $t\alpha^+$ and $t\alpha^-$ which are the values corresponding to the half wells W^+ and W^- , respectively.

At this stage, it is informative to determine those temperatures at which either α^+ or α^- vanishes. Let t_0^+ and t_0^- be the temperatures such that $\alpha^+(t_0^+) = \alpha^-(t_0^-) = 0$ hold. Using (28), one can immediately determine t_0^{\pm} as

$$t_0^+ = \frac{2N}{\pi^2}, \quad t_0^- = \frac{6N}{\pi^2}. \quad (31)$$

One then finds, numerically,

$$t_0^+ \alpha^-(t_0^+) = -0.7627, \quad t_0^- \alpha^+(t_0^-) = 0.9026. \quad (32)$$

Our assumptions $b \ll 1$ and $|\alpha^\pm| \ll 1$ are in fact valid at these temperatures, since we have $t_0^\pm \sim N \gg 1$ and $\alpha_0^\pm \sim 1/t = b \sim 1/N \ll 1$. Obviously, the same will apply for the temperatures between and in the neighborhood of these two values t_0^\pm . Moreover, we can expect from these results that, for $t \sim N$ in general,

$$\alpha^\pm \sim b \sim 1/N \ll 1. \quad (33)$$

In what follows, we shall be interested in this temperature regime, where the minimum of the force difference Δf_{\min} is found in the numerical result (see Fig. 4). One can show — see Appendix B for the details — that, for $t \sim N$, the relative error of our approximation (26) decreases with increasing N .

Next, we derive an approximated analytical expression for the net force Δf obtained under (33). We do this with the help of an integral approximation for the force sums. Presenting all the technical details of the calculation in Appendix B, here we summarize only the result,

$$\frac{\Delta f}{N} \approx -\frac{1}{2} \frac{t}{N} - \Delta(t\alpha). \quad (34)$$

This formula has a relative error that tends to vanish in the large- N limit.

We observe from (34) that, in this medium temperature domain, $\Delta f/N$ is also a function of t/N as $t\alpha$ is. Consequently, the force curve $\Delta f(t)$ is scale invariant in N (*i.e.*, it preserves its shape under the rescaling of N) as both the effective range of t and Δf scale linearly with N . As a special case, we see that the temperature of the minimum force occurs at $t_{\min} \sim N$, $\Delta f_{\min} \sim N$, confirming our observation made in the numerical analysis in Fig. 4.

Let us now determine the ratios t/N and $\Delta f/N$ in the large- N limit. One possible way to do this is to use various values of t/N to solve numerically (30) for α and insert the outcomes into (34), and thereby reproduce the force curve at those values. For example, the minimum of $\Delta f/N$ as the function of t/N can be estimated in this way, yielding the ratios

$$\frac{t_{\min}}{N} \approx 0.5480, \quad \frac{\Delta f_{\min}}{N} \approx 0.5967. \quad (35)$$

These values agree with the numerical results pretty well as readily confirmed in Fig. 4.

To find an analytical formula for Δf as well, one may use some expansion approximation of the functions S^\pm (see Eq. 28) around some chosen value. As an example, let us choose t to be in the vicinity of t_0^- . There, $|t\alpha^-| \ll 1$, and the equation we wish to solve becomes

$$\begin{aligned} \frac{N}{t} &= \frac{\pi\sqrt{t\alpha^-} \coth \pi\sqrt{t\alpha^-} - 1}{2t\alpha^-} \\ &= \frac{\pi^2}{6} - \frac{\pi^4}{90}t\alpha^- + \frac{\pi^6}{945}(t\alpha^-)^2 + \mathcal{O}\left((t\alpha^-)^3\right). \end{aligned} \quad (36)$$

Inverting this, one can obtain the solution as

$$t\alpha^- = \frac{5}{2}\left(\frac{t}{N} - \frac{6}{\pi^2}\right) + \frac{5\pi^2}{28}\left(\frac{t}{N} - \frac{6}{\pi^2}\right)^2 + \mathcal{O}\left(\left(\frac{t}{N} - \frac{6}{\pi^2}\right)^3\right). \quad (37)$$

As for $t\alpha^+$, we observe that it is close to the value 0.9 [see (32)], where $\pi\sqrt{t\alpha^+} \approx 3$ and $\tanh \pi\sqrt{t\alpha^+}$ already almost saturates to its large-variable asymptotic value, 1. Taking this simple asymptotic approximation,

$$\tanh \pi\sqrt{t\alpha^+} \approx 1, \quad (38)$$

one can determine $t\alpha^+$ by the solution of $N/t = \pi/(2\sqrt{t\alpha^+})$, that is,

$$t\alpha^+ = \frac{\pi^2}{4}\left(\frac{t}{N}\right)^2. \quad (39)$$

Applying the solutions (37) and (39) in (34) yields

$$\frac{\Delta f}{N} \approx \frac{\pi^2}{14}\left(\frac{t}{N} - \frac{6}{\pi^2}\right)^2 + \frac{6}{\pi^2}. \quad (40)$$

This quadratic formula (40) indicates that the location of the minimum occurs at

$$\frac{t_{\min}}{N} \approx \frac{\Delta f_{\min}}{N} \approx \frac{6}{\pi^2} = 0.6079\dots. \quad (41)$$

Fig. 4 shows that around the minimum the formula (40) reproduces the numerical curve of the force reasonably well.

To improve our formula to achieve a better agreement between (41) and (35), we consider the approximation:

$$\tanh x \approx \frac{\tanh x^* + (x - x^*)}{1 + \tanh x^* \cdot (x - x^*)}. \quad (42)$$

This formula is precise up to the quadratic Taylor term at x^* , and behaving much better than the quadratic Taylor polynomial approximation in a larger neighborhood. For the expansion point $x^* \equiv \pi\sqrt{(t\alpha^+)^*}$, we may simply choose the above-mentioned value, 3. Using the notation $t^*/N := S^+((t\alpha^+)^*)$ — which is close to t_0^-/N — and assuming an expansion of the form

$$t\alpha^+ - (t\alpha^+)^* = c_1 \left(\frac{t}{N} - \frac{t^*}{N} \right) + c_2 \left(\frac{t}{N} - \frac{t^*}{N} \right)^2 + \mathcal{O} \left(\left(\frac{t}{N} - \frac{t^*}{N} \right)^3 \right), \quad (43)$$

we obtain a quadratic approximation for $t\alpha^+$ that is better than (39). Accordingly, the force difference is obtained in the improved form,

$$\frac{\Delta f}{N} \approx 0.5121 \cdot \left(\frac{t}{N} - 0.5465 \right)^2 + 0.5967, \quad (44)$$

having its minimum at

$$\frac{t_{\min}}{N} \approx 0.5465, \quad \frac{\Delta f_{\min}}{N} \approx 0.5967. \quad (45)$$

We remark that the parabolic approximation used above is valid only locally and not suitable for describing the whole medium temperature domain. To find a formula valid for other values of temperatures, we may simply expand at the value of the interest and/or using approximate formulas for the other parts of the functions S . A more universally valid approximate formula, which describes the force curve in the whole medium temperature region, is obviously desirable but it is rather difficult to find at the moment.

4.2 Fermions

The numerical results shown in Fig. 4 suggest that, for fermions, the medium temperature regime that includes the temperature of the minimum force may be defined as the domain where $t \sim N^2$, $\Delta f \sim N^2$ are fulfilled. Now we investigate this regime to seek an analytic approximation of the force curve there.

As we did for the bosonic case, we first determine α . Our integral approximation presented in Appendix B gives

$$N = \sum_{n=1}^{\infty} \frac{1}{e^{\alpha+y_n^2} + 1} \approx \frac{\tau - 1/2}{e^{\alpha} + 1} + \frac{1}{\sqrt{b}} I(\alpha) \quad (46)$$

with the Fermi-Dirac integral $I(\alpha)$ given by

$$I(\alpha) := \int_0^\infty \frac{dy}{e^{\alpha+y^2} + 1}. \quad (47)$$

Since $\frac{1}{e^\alpha + 1} \approx N_1 < 1$, for large N we can simplify (46) to

$$N \approx \sqrt{t} I(\alpha) \quad \text{or} \quad t \approx \frac{N^2}{I(\alpha)^2}, \quad (48)$$

where, for temporary convenience, we solve our condition for t as a function of α , instead of the reverse. We observe that $t \sim N^2$ implies $\alpha = \mathcal{O}(N^0)$, unlike in the medium temperature regime of the bosonic case.

Since there arises no difference between α^+ and α^- in this leading order, we need to consider the subleading term for $\Delta\alpha$. This can be derived from (46) as

$$0 = \Delta N \approx \Delta \left[\frac{\tau - \frac{1}{2}}{e^\alpha + 1} \right] + \frac{1}{\sqrt{b}} I'(\alpha) \Delta\alpha, \quad \Delta\alpha \approx \frac{1}{2N} \frac{I(\alpha)}{(e^\alpha + 1) I'(\alpha)}, \quad (49)$$

where we have used the fact that, in leading order, the difference between α^+ or α^- can be ignored (and we have again eliminated t as a function of α).

For the force, our integral approximation provides

$$f = \sum_{n=1}^\infty \frac{e_n}{e^{\alpha+y_n^2} + 1} = b^{-3/2} \sum_{n=1}^\infty \frac{y_n^2 \Delta y}{e^{\alpha+y_n^2} + 1} \approx \mathcal{O}(t^0) + t^{3/2} \int_0^\infty \frac{y^2 dy}{e^{\alpha+y^2} + 1}, \quad (50)$$

and hence by integration by parts and (49) we obtain

$$\Delta f \approx t^{3/2} \int_0^\infty \frac{-e^{\alpha+y^2} \Delta\alpha}{(e^{\alpha+y^2} + 1)^2} y^2 dy = \frac{-t^{3/2}}{2} \Delta\alpha \int_0^\infty \frac{dy}{e^{\alpha+y^2} + 1} \approx \frac{N^2}{4} J(\alpha), \quad (51)$$

with

$$J(\alpha) := \frac{-1}{(e^\alpha + 1) I(\alpha) I'(\alpha)} = \frac{-2}{(e^\alpha + 1) dI^2(\alpha)/d\alpha}. \quad (52)$$

All these approximations will improve for larger values of t and N . We can see in (51) that, having $\alpha = \mathcal{O}(N^0)$, not only t but also Δf scale with N^2 in the

medium temperature regime, and consequently the force curve is again scale invariant in N (shape-preserving under rescaling N) in this regime.

As before, for a given t , one can obtain α and Δf by solving a transcendental equation numerically or by using some analytical approximate formula. For instance, determining the location of the minimum — in essence, the minimum of $J(\alpha)$ — via numerical solution, one finds

$$\alpha_{\min} = -2.567, \quad J(\alpha_{\min}) \approx 1.813, \quad t_{\min} \approx 0.444N^2, \quad \Delta f_{\min} \approx 0.453N^2. \quad (53)$$

These values are in apparent accord with the fully numerical results in Fig. 4.

For an analytical approach, first one can take the standard asymptotic series for the Fermi-Dirac integral $I(\alpha)$. According to [14], in the interval $\alpha \in [-3.696, -1.314]$ the truncation

$$I(\alpha) \approx \sqrt{-\alpha} \left[1 - \frac{\pi^2}{24} \frac{1}{(-\alpha)^2} \right] \quad (54)$$

of the asymptotic series is the best available approximation for $I(\alpha)$. Unfortunately, this is not sufficient for our purpose because the approximated $J(\alpha)$ obtained from this does not possess a minimum. However, noticing that, for $I'(\alpha)$, a better approximation is obtained by the further truncated

$$I'(\alpha) \approx \frac{1}{2\sqrt{-\alpha}} \quad (55)$$

we can find, using this in $J(\alpha)$, a minimum in the temperature regime we are considering. By numerically solving the arising transcendental equation, one finds

$$\alpha_{\min} \approx -1.95, \quad J(\alpha_{\min}) \approx 1.96, \quad t_{\min} \approx 0.611N^2, \quad \Delta f_{\min} \approx 0.49N^2, \quad (56)$$

which are not quite precise compared to (53).

To find a second, better approximation of $I(\alpha)$, we utilize the fact that its integrand, $\frac{1}{e^{\alpha+y^2}+1}$ is close to a tangent hyperbolic function (reflected and shifted) on $y \in [0, \infty)$, for negative α . Specifically, we may write

$$\begin{aligned} I(\alpha) &\approx \int_0^\infty \frac{p}{2} \left[1 - \tanh \sqrt{-\alpha} (y - \sqrt{-\alpha}) \right] dy \\ &= \frac{p}{2\sqrt{-\alpha}} \left[-2\alpha + \ln(1 + e^{2\alpha}) \right] \end{aligned} \quad (57)$$

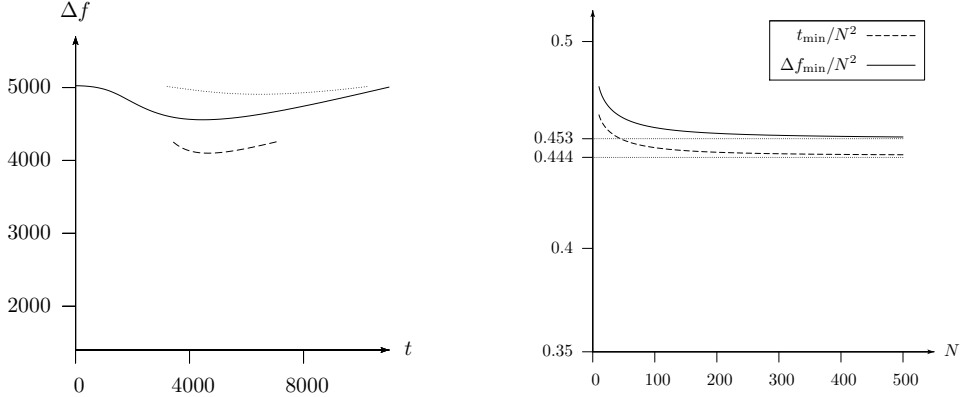


Fig. 6. (Left) The minimum of the force curve for fermions, at $N = 100$. Solid line: numerical computation; dotted line: the approximation corresponding to (56); dashed line: the approximation corresponding to (60). (Right) the scaling behavior of t_{\min} and Δf_{\min} . The constants determined at (53) are also displayed.

with $p := \frac{1+e^{2\alpha}}{1+e^\alpha}$. Here, the integrand is chosen to be simple enough but still to reproduce the true integrand exactly at $y = 0$ and decreases to the half of the $y = 0$ value around the same point with similar steepness. Omitting $\mathcal{O}(e^{4\alpha})$ terms can reduce the obtained formula to

$$I(\alpha) \approx \frac{p}{2\sqrt{-\alpha}} (-2\alpha + e^{2\alpha}), \quad I^2(\alpha) \approx p^2 (-\alpha + e^{2\alpha}). \quad (58)$$

Since no further available simplification can render the resulting transcendental equation analytically solvable for α , we shall use (58) to expand our $J(\alpha)$ approximation around, say, $\alpha^* = -2.5$ to second order, and determine the minimum of the quadratic Taylor polynomial, which polynomial we can rewrite in the form

$$J(\alpha) \approx 0.134(\alpha + 2.48)^2 + 1.64. \quad (59)$$

This way we reach

$$\alpha_{\min} \approx -2.48, \quad J(\alpha_{\min}) \approx 1.64, \quad t_{\min} \approx 0.466N^2, \quad \Delta f_{\min} \approx 0.411N^2, \quad (60)$$

which agree better with the numerical results; see (53) and Fig. 4. Should one need a further improved formula, the approach can be repeated with some enhanced or more diligent choice for approximating the integrand in $I(\alpha)$.

5 Low temperature regime

Having analyzed the quantum force on the partition in high and medium temperature regimes, we now consider the force under low temperatures in this section.

5.1 Bosons

To discuss the bosonic case, let us first approach from the zero-temperature end. Since at exactly zero temperature all the particles sit on the lowest available level which is the ground state for bosons, we immediately obtain

$$f^+(0) = e_1^+ N = \frac{N}{4}, \quad f^-(0) = e_1^- N = N. \quad (61)$$

This implies

$$\Delta f(0) = \frac{3}{4}N, \quad (62)$$

which is nonzero and is proportional to N .

When the temperature is slightly above zero, the particles occupy the lower excited levels in addition to the ground state, and the transition from the ground level to the upper levels is more extensive in the half well W^+ than W^- , because the subsequent energy levels have a smaller difference in W^+ than W^- (see (5)). Consequently, the force difference will decrease as t grows from zero. Indeed, in the two-level approximation for bosons, where the higher levels are treated as still completely unoccupied, the net force is found to be [10]

$$\Delta f(t) \approx \frac{3}{4}N + (3e^{-3/t} - 2e^{-2/t}), \quad (63)$$

which accounts for decrease, see Fig. 7. Note that $\Delta f(t)$ starts to decrease for $t \sim 1$, irrespective of the particle number N . Incidentally, we mention that the low temperature behavior for α is

$$\alpha \approx -be_1 + \ln \left(1 + \frac{1}{N} \right), \quad (64)$$

which is a straightforward consequence of the approximation $N_1 \approx N$.

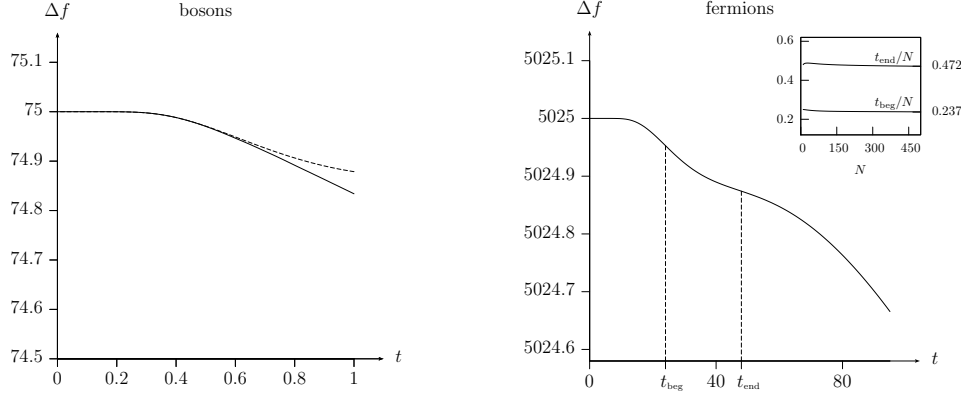


Fig. 7. The low-temperature behavior of the net force Δf , for $N = 100$. (Left) the bosonic case. Solid line: numerical computation, dashed line: the two-level approximation (63). (Right) the numerical results for the fermionic case. Observe the steplike shape, characterized by the temperature values at the two points of inflection. The inset displays t_{beg}/N and t_{end}/N , as the function of N . They appear to tend to constants that are approximately 0.237 and 0.472, respectively. Within an error, the second number is just the double of the first one.

5.2 Fermions

To study the zero temperature limit for fermions, we recall that the lowest N levels are occupied at $t = 0$, and from this we obtain

$$f^+(0) = \sum_{n=1}^N e_n^+ = \frac{N(4N^2 - 1)}{12}, \quad f^-(0) = \sum_{n=1}^N e_n^- = \frac{N(N + 1)(2N + 1)}{6}, \quad (65)$$

which implies

$$\Delta f(0) = \frac{N(2N + 1)}{4}. \quad (66)$$

Observe that, in contrast to the bosonic case, the force difference in the fermionic case is (for $N \gg 1$) proportional to N^2 in the limit $t \rightarrow 0$.

We have learned that the fermionic net force $\Delta f(t)$ differs from the bosonic one quantitatively in the zero temperature limit $\Delta f(0)$ — it is proportional to N^2 for fermions while the order is N for bosons. Another quantitative difference can be observed in the first ‘turning point’, namely the temperature where $\Delta f(t)$ starts to decrease when the temperature t is increased from zero — the turning point occurs at around $t \sim N$ for fermions (as confirmed numerically) while it occurs at around $t \sim 1$ for bosons. Besides, there is a qualitative difference between the fermionic and the bosonic cases — the fermionic curve

exhibits a single, very small but unmistakable ‘steplike’ pattern (or a depression) for any N during the initial decrease as shown in Fig. 8. This step occurs at a temperature proportional to N (see Fig. 8), and the net force differs there from the $\mathcal{O}(N^2)$ zero temperature value by only an $\mathcal{O}(N^0) = \mathcal{O}(1)$ amount.

These numerically observed properties can be understood analytically as follows. For fermions, the analogue of the bosonic two-level approximation corresponds to the situation where only the occupation of the N th and $(N+1)$ th levels (*i.e.*, the two levels closest to the Fermi level) are different from the zero temperature value. On each side, this imposes the approximate equation

$$N_N + N_{N+1} = 1, \quad N_{N+1} = \frac{1}{e^{\alpha+be_{N+1}} + 1} = 1 - N_N = \frac{1}{e^{-\alpha-be_N} + 1}, \quad (67)$$

which can be solved for α as

$$\alpha \approx -\frac{b}{2} (e_N + e_{N+1}). \quad (68)$$

Let us observe that, with this approximation for α ,

$$N_{N+l} = \frac{1}{e^{\alpha+be_{N+l}} + 1} \approx 1 - N_{N+1-l} = \frac{1}{e^{-\alpha-be_N} + 1} \approx \frac{1}{e^{(2l-1)bN} + 1} \quad (69)$$

($l = 1, 2, \dots$) in the leading order of N in the exponents. Keeping only two nontrivial levels for calculating the forces as well (*i.e.*, $l = 1$ only), we have

$$\begin{aligned} f &= \sum_{n=1}^{\infty} e_n N_n = \sum_{n=1}^N e_n + \sum_{n=1}^N e_n (1 - N_n) + \sum_{n=N+1}^{\infty} e_n N_n \\ &\approx f(0) + (e_{N+1} - e_N) N_{N+1}. \end{aligned} \quad (70)$$

At this point, we observe that a cancellation in the leading order of N takes place, since we have $e_N \approx e_{N+1} \approx N^2$ but $e_{N+1} - e_N = 2N + (1 - 2\tau)$ (and, in general, $e_{N+l} - e_{N+1-l} = (2l-1)[2N + (1 - 2\tau)]$) with τ used in (28), which is only $\mathcal{O}(N)$. An even higher cancellation will occur in the force difference, as this leading $\mathcal{O}(N)$ difference is the same on the two sides and, according to (69), N_{N+1} is also the same on the two sides in the leading order of N . To obtain a nonvanishing contribution, we use for N_{N+1}^{\pm} the first-order Taylor approximation

$$\frac{1}{e^{X+\Delta X} + 1} \approx \frac{1}{e^X + 1} - \frac{e^X}{(e^X + 1)^2} \Delta X \quad (71)$$

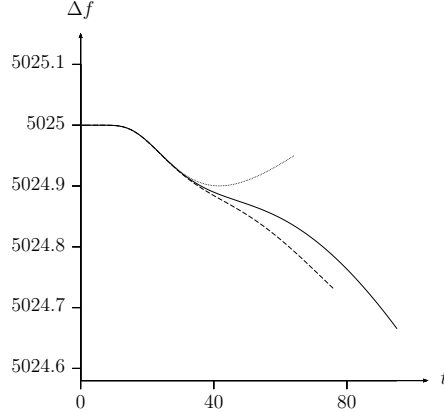


Fig. 8. The two- and semi-four-level approximations (dotted and dashed lines, respectively) near the fermionic step (solid line) for $N = 100$.

with $X = bN$ and appropriate ΔX^\pm . This gives

$$\begin{aligned} \Delta f &\approx \Delta f(0) + \frac{1}{e^{bN} + 1} - b \left(N + \frac{1}{2} \right) \frac{e^{bN}}{(e^{bN} + 1)^2} \\ &\approx \Delta f(0) + \frac{1}{e^{bN} + 1} - bN \frac{e^{bN}}{(e^{bN} + 1)^2}. \end{aligned} \quad (72)$$

Now we can see that this last expression contains t only in the combination $bN = N/t$, which explains why the decrease of the net force from the zero temperature value starts at $t \sim N$. Further, it is also visible that this decrease at $t \sim N$ is only a small $\mathcal{O}(N^0) = \mathcal{O}(1)$ phenomenon.

This two-level approximation is not sufficient to explain the step in the curve pertinent to the fermionic case (see Fig. 8). However, we may apply a semi-four-level approximation, that is, we assume four nontrivially occupied levels but use the two-level-approximated α . The net force evaluated by an analogous procedure then becomes

$$\Delta f \approx \Delta f(0) + \frac{1}{e^{bN} + 1} + \frac{3}{e^{3bN} + 1} - \frac{bN e^{bN}}{(e^{bN} + 1)^2} - \frac{13bN e^{3bN}}{(e^{3bN} + 1)^2}. \quad (73)$$

From this, we are able to read off t_{beg} and t_{end} that characterize the location of the step in Fig. 8 by numerically determining the points of inflection as a function of t/N . The results

$$t_{\text{beg}}/N \approx 0.239, \quad t_{\text{end}}/N \approx 0.426 \quad (74)$$

are indeed close to the numerically observable values 0.237 and 0.472, respectively.

However, as seen in Fig. 8, for the curve over the entire low temperature regime, this semi-four-level approximation is less satisfactory. Our further investigation shows that the net force Δf is extremely sensitive to the error in α , and that incorporating two more levels provides only a smaller contribution compared to the change caused by the error. It seems, therefore, that a full four-level approximation for α is required for the net force to reproduce the numerical curve more precisely.

6 The partition shift Δl and the transfer number ΔN

We have seen that the quantum effect caused by a set of nontrivial boundary conditions manifests in the force that arises on the partition in a potential well. For actual observation of the effect, however, there may be other quantities which are more readily measurable than the force itself. In this section we mention briefly two examples of such quantities: the shift Δl in the position of the partition and the transfer ΔN of particles between the two half wells (see Fig. 9). For simplicity, our discussions are mostly restricted to the zero temperature limit $t \rightarrow 0$.

To discuss the first example, suppose that the partition is allowed to move freely in the well. Due to the pressure, the partition will then move and accordingly the widths of the half wells W^\pm change as

$$W^+ : l \rightarrow l(1 - \xi), \quad W^- : l \rightarrow l(1 + \xi), \quad (75)$$

so that the net force vanishes, $\Delta F(0) = 0$. The portion ξ of the shift $\Delta l = l\xi$ is thus determined by

$$0 = \Delta F(0) = \frac{(\hbar\pi)^2}{m} \frac{1}{l^3} \left[\frac{f^-(0)}{(1 + \xi)^3} - \frac{f^+(0)}{(1 - \xi)^3} \right]. \quad (76)$$

From this we find

$$\xi = \frac{r - 1}{r + 1} \quad \text{with} \quad r = \left[\frac{f^-(0)}{f^+(0)} \right]^{1/3}. \quad (77)$$

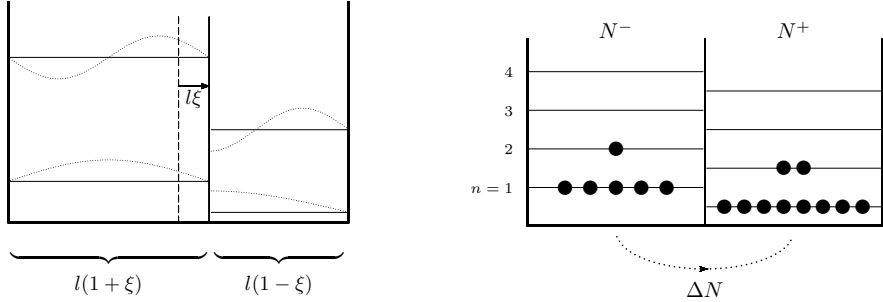


Fig. 9. (Left) the shift $\Delta l = l\xi$ in the position of the partition. (Right) the redistribution of particles $\Delta N = N_+ - N_-$. Both Δl and ΔN are determined from the stability, $\Delta F(0) = 0$.

For the bosonic case, (62) implies $r = \sqrt[3]{4}$ and hence

$$\xi = \frac{\sqrt[3]{4} - 1}{\sqrt[3]{4} + 1} \simeq 0.227. \quad (78)$$

This shows that the shift is rather large reaching nearly a quarter of the original width. Notice that for the bosonic case the portion ξ of the shift is independent of the particle number N .

For the fermionic case, in contrast, the force limit (66) implies the factor $r \simeq 1 + 1/(2N)$ for $N \gg 1$ to each up and down spin, and hence the portion ξ in (77) becomes

$$\xi \simeq \frac{1}{4} \frac{1}{N}, \quad (79)$$

which is quite small for large N (*e.g.*, less than 1 percent even for $N = 100$). The result (79) indicates that the fermionic shift is much smaller than the bosonic one (78) and is almost undetectable for large N . We thus learn that the spread of particles over the levels according to the Fermi-Dirac statistics has the effect of balancing the partition near the center.

When the temperature t increases from zero, the shift ξ decreases steadily for all t in both bosonic and fermionic cases. This is due to the fact that as t becomes higher the forces f^- and f^+ grow faster than their difference, rendering the ratio r closer to unity. This is seen clearly in our numerical analysis shown in Fig. 10. Interestingly, it also shows that, for fermions for instance, the turning point of the shift ξ after the initial plateau in the vicinity of $t = 0$ has a curious scaling property under the change of the particle number N . Namely, the inset of Fig. 10 indicates that the turning point temperature of ξ depends linearly on N (since, for $N\xi$, it scales as N^2), which is the same

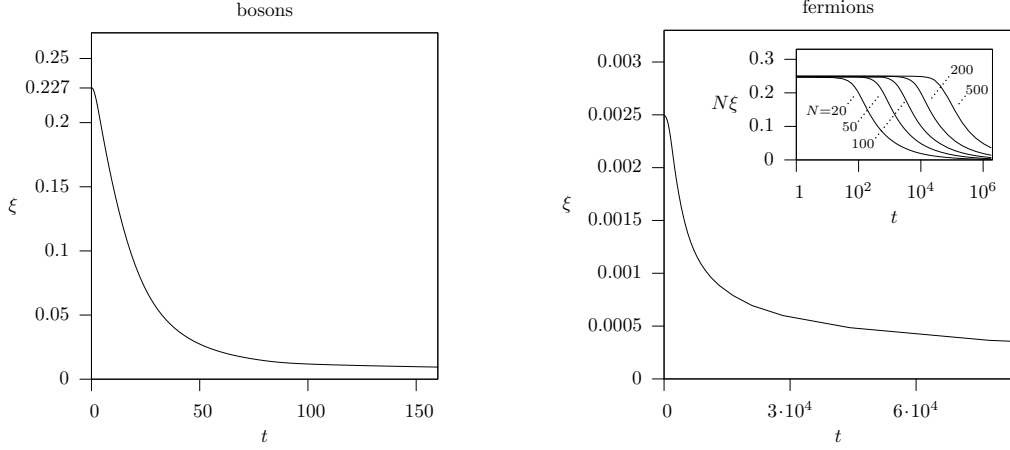


Fig. 10. The equilibrial shift of the partition as the function of temperature obtained numerically for $N = 100$; (Left) for bosons and (Right) for fermions. The inset in the fermionic case shows the quadratic N -dependence of the combination $N\xi(t)$.

scaling law found for the force Δf for its turning point in the low temperature regime.

In our second example, we suppose that unlike in the previous situation the partition is fixed firmly at the center but instead we consider to move particles from one half well to the other until the equilibrium $\Delta F(0) = 0$ is achieved. Let N_+ and N_- be the redistributed number of particles in the half wells W^\pm , *i.e.*,

$$W^+ : N \rightarrow N_+, \quad W^- : N \rightarrow N_-, \quad \text{with} \quad N_+ + N_- = 2N. \quad (80)$$

The amount $\Delta N = N_+ - N$ of moved particles with respect to the original numbers N is another good measure of how far the original situation is away from the mechanical equilibrium. The condition to determine this number ΔN is just $r = 1$ with r given in (77).

For the bosonic case, where we have (61), this condition implies $N_+/(4N_-) = 1$ and, accordingly, the stability is achieved by the ratio

$$\frac{N_+}{N_-} = 4. \quad (81)$$

Thus the redistributed numbers read

$$N_+ = \frac{8}{5}N \quad \text{and} \quad N_- = \frac{2}{5}N, \quad (82)$$

which implies that a large portion (60%) of particles must be moved from

one well to the other to achieve the equilibrium. As in the previous example, this portion does not depend on the particle number N . This second example also illustrates the fact that the bosonic case is macroscopically far from the mechanical equilibrium and hence the effect may easily be observed experimentally.

In contrast, the fermionic case has the limit (66), and the equilibrium condition $r = 1$ implies $(N_+/N_-)^3 \cdot (1 + 3/(2N_-))^{-1} = 1$. This is achieved with the ratio,

$$\frac{N_+}{N_-} \simeq 1 + \frac{1}{2} \frac{1}{N_-} \quad (83)$$

The outcome shows that the instability caused by the net force on the partition is extremely small so that even the redistribution by a single particle from W^- to W^+ can reverse the instability ($\Delta F(0) < 0$). We thus learn that, in terms of redistribution, the effect of the quantum force on the partition is almost invisible for the fermionic case. Again, we see that the fermionic setting is macroscopically close to the mechanical equilibrium.

7 Conclusion and Discussions

In the present paper, we have investigated physical consequences of nontrivial boundary conditions in a quantum well realized by a partition placed at the center of the well. We have examined the pressure appearing on the partition due to the distinct boundary conditions on the two sides (Dirichlet on the left and Neumann on the right), taking into account of the thermal effects under finite temperatures as well as the different statistics of the particles in the well. We have found that, for both bosons and fermions, the net force $\Delta f(t)$ acting on the partition in the quantum well is nonzero at the zero temperature limit $t \rightarrow 0$, and remains practically constant for extremely low temperatures before it starts to decrease gradually for higher (but still low) temperatures. Knowing that the energy spectrum is different in the two half wells W^- and W^+ separated by the partition for all energy regimes, this property is not unexpected. What is unexpected, however, is that this decrease stops at a certain temperature t_{\min} and afterwards the net force increases persistently up to the high temperature limit $t \rightarrow \infty$ where it diverges according to the square root of the temperature \sqrt{t} .

We have also observed a salient scaling property in the particle number N , that is, the force is of the order of N for the bosonic case while it is of the order of N^2 . Furthermore, the minimal force Δf_{\min} and the minimal temperature t_{\min} follow the same scaling law, *i.e.*, they are both of the order of N for bosons and N^2 for fermions. These properties are found numerically and have

also been successfully reproduced by analytical approximations developed in this paper. This curious scaling dependence pertinent to the particle statistics may be widely observed in other physical phenomena, not just in the quantum force we have studied. The shift of the partition mentioned in the previous section can be one such example.

The difference in the scaling does not necessarily imply that the quantum force is more easily measured for the fermionic case than the bosonic case. In fact, we have seen in the (imaginative) shift in the partition or the redistribution of particles caused by the force that the effect of the force in these quantities is rather marked in the bosonic case while it is almost invisible for the fermionic case.

Compared to the bosonic case, the fermionic case admits an additional property: for low temperatures the force exhibits a subtle step-like pattern, a small dent, just after it starts to decrease from the constant plateau in the extremely low temperature regime. This property has also been reproduced by analytical approximations, at least semiquantitatively.

From the expectation that all the effects that arise from quantum boundary conditions should vanish at high temperatures where the classical picture would be available, the observed divergence of the force seems quite unusual. However, this may be understood by the fact that, contrary to most quantum systems in higher dimensions, one dimensional quantum wells possess energy spectra with increasing level spacing for higher energy levels (which is actually valid not only for wells with Dirichlet and/or Neumann boundary conditions but also for all other wells as well [16]). In other words, the dimensionality of quantum wells can be examined by their high-temperature behavior, too. In actual realizations of the well, there is of course a maximal height of the potential, which will modify the high-temperature behavior and eventually assimilate it to the classical one in the limit $t \rightarrow \infty$.

The calculation presented here could be performed for other, more general boundary conditions. For most boundary conditions, however, the energy levels will be determined by transcendental equations and, accordingly, additional technical difficulties, especially analytical ones, will arise. In this respect, the present combination by the Dirichlet and Neumann conditions is certainly special in that it admits a simple and yet distinct set of energy levels for the two half wells. Nevertheless, one may expect that, in this example where the two ‘extreme’ boundary conditions are used, most of the generic features that could arise from nontrivial boundary conditions have appeared. We hope that the present study furnishes an intimate picture of the effect of boundary conditions in quantum mechanics, paving the way toward fuller understandings of quantum singularities in general.

Acknowledgement: This work is supported by the Grant-in-Aid for Scientific Research, No. 13135206 and No. 16540354, of the Japanese Ministry of Education, Science and Culture.

A Outline of the numerical calculation of the net force

The purely numerical computation of the net force Δf for a given particle number N and temperature t used in this paper is performed in the following scheme. First, in each half well, we solve the total number condition (9) for α , then substitute the obtained α into the corresponding expression (11) for the force f , and at last we take the difference of the two forces f^- and f^+ . We have to control errors coming from three sources. The first is that we use finite truncations of the involved infinite sums, the second is that we obtain α via a numerical solution of the number condition, and the third is the floating-point errors of the calculations.

For a prescribed precision of the force f , we estimate the required precision in α by taking the partial derivative of the sum (11) with respect to α at a fixed temperature parameter b . Similarly, the derivative of the sum (9) with respect to α is used to find the corresponding precision at which (9) has to be fulfilled when seeking for the solution α .

When setting this required precision, we also incorporate the error of the truncation of the infinite sums we face at, *i.e.*, of (9), (11), and their mentioned derivatives. To this end, simple upper estimate formulas for the dropped infinite terms are derived. For low temperatures, we can estimate from above by some appropriate geometric series $\sum_{n=n_{\text{trunc}}}^{\infty} q^n$ or its generalization $\sum_{n=n_{\text{trunc}}}^{\infty} (c_2 n^2 + c_1 n + c_0) q^n$, which is summable in closed form. In parallel, for high temperatures, it is better to replace any dropped discrete sum with a corresponding continuous integral (cf. (B.1)–(B.3)). Then we change the integrand to a simpler upper bound of it, to reach an integral like $\int_{y_{\text{trunc}}}^{\infty} e^{-y^2} dy$. Finally, we employ the standard approximate closed expressions to evaluate this simpler definite integral (the first few terms of its large- y_{trunc} expansion).

The floating-point precision must also be chosen appropriately. The number of floating-point digits must be such high that a further increase in the number of digits influences the force difference result well within the uncertainty we prescribed for it. Unsurprisingly, we find that higher temperature t and larger particle number N require better floating-point precision. One should use such a mathematical computer software that allows to have 20 digits or more. Our calculations have been performed using Maple (© Maplesoft, Waterloo Maple Inc.).

B Calculations for the medium temperature regime

For both the bosonic and the fermionic case, we will make use of an integral approximation of the infinite sums. Namely, the trapezoid approximation of integrals, applied for a function $g(y)$ behaving ‘peacefully’ in $[y_1, \infty)$ with $\lim_{y \rightarrow \infty} g(y) = 0$, yields

$$\sum_{n=1}^{\infty} g(y_n) \approx \frac{g(y_1)}{2} + \frac{1}{\Delta y} \int_{y_1}^{\infty} g(y) \, dy, \quad (\text{B.1})$$

for constant intervals $\Delta y = y_{n+1} - y_n = \text{const.}$ This approximation improves for smaller Δy . Remarkably, the trapezoid approach provides an approximation one order better (in Δy) than the simple rectangular one.

Now, in all our applications used in the text, we have

$$y_n = \sqrt{be_n} = \sqrt{b}(n - \tau), \quad \Delta y = \sqrt{b} \quad (\text{B.2})$$

for a constant τ (defined as $\tau = \frac{1}{2}$ for W^+ and $\tau = 0$ for W^- in (29)). If g is ‘peaceful’ even in $[0, \infty)$, which will always be the case here, then we have further

$$\begin{aligned} \sum_{n=1}^{\infty} g(y_n) &\approx \frac{g(y_1)}{2} - \frac{y_1}{\Delta y} g(0) + \frac{1}{\Delta y} \int_0^{\infty} g(y) \, dy \\ &\approx \underbrace{\left(\frac{1}{2} - \frac{y_1}{\Delta y} \right)}_{\tau-1/2 \text{ in our case}} g(0) + \frac{1}{\Delta y} \int_0^{\infty} f(y) \, dy. \end{aligned} \quad (\text{B.3})$$

In the main body of the present paper, wherever a sum is approximated by an integral, we have used (B.3).

Let us consider the bosonic case where we have $t \sim N$ in the medium temperature region. There, we can show that the relative error of the approximation (26) tends to zero in the large- N limit. Indeed,

$$\frac{1}{N} \sum_{n=1}^{\infty} \left[\underbrace{\frac{1}{e^{\alpha+y_n^2} - 1} - \frac{1}{\alpha + y_n^2}}_{-\frac{1}{2} + \frac{\alpha+be_n}{12} + \mathcal{O}((\alpha+be_n)^3)} \right]$$

$$\begin{aligned}
&\approx \frac{1}{N} \left\{ \frac{1-2\tau}{4} \left(1 - \frac{\alpha}{6} \right) + \frac{1}{\sqrt{b}} \int_0^\infty \left(\frac{1}{e^{\alpha+y^2} - 1} - \frac{1}{\alpha + y^2} \right) dy \right\} \\
&\approx \frac{1}{N} \left\{ \mathcal{O}(N^0) + \mathcal{O}(N^{1/2}) \right. \\
&\quad \left. \times \left[\underbrace{\int_0^\infty \left(\frac{1}{e^{y^2} - 1} - \frac{1}{y^2} \right) dy}_{-1.2942} t + \underbrace{\int_0^\infty \left(\frac{1}{y^4} - \frac{e^{y^2}}{(e^{y^2} - 1)^2} \right) dy}_{0.1842} \alpha \right] \right\}, \tag{B.4}
\end{aligned}$$

which is altogether an $\mathcal{O}(N^{-1/2})$ quantity, vanishing in the limit $N \rightarrow \infty$.

Next, we derive (34) and its order of relative error, under the conditions $b \sim 1/N \ll 1$ and $|\alpha^+|, |\alpha^-| \sim 1/N \ll 1$. For the force on one side, we can write

$$f = \sum_{n=1}^{\infty} \frac{e_n}{e^{\alpha+be_n} - 1}, \quad bf + N\alpha = \sum_{n=1}^{\infty} \frac{\alpha + be_n}{e^{\alpha+be_n} - 1} = \sum_{n=1}^{\infty} \frac{z_n}{e^{z_n} - 1} \tag{B.5}$$

with $z_n := \alpha + be_n$. Thus, for the force difference, we have

$$\begin{aligned}
\Delta(bf + N\alpha) &= b\Delta f + N\Delta\alpha = \sum_{n=1}^{\infty} \Delta \left(\frac{z_n}{e^{z_n} - 1} \right) \\
&\approx \sum_{n=1}^{\infty} \left(\frac{d}{dz} \frac{z}{e^z - 1} \right)_{z=z_n} \cdot \Delta z_n. \tag{B.6}
\end{aligned}$$

Note that in the sum (B.6), the factor

$$\Delta z_n = z_n^- - z_n^+ = \Delta\alpha + b\Delta(n - \tau)^2 = \Delta(\alpha + b\tau^2) - 2b\Delta\tau n \tag{B.7}$$

is small $\Delta z_n = \mathcal{O}(N^{-1/2})$ up to $n = \mathcal{O}(t^{1/2})$, while the higher n terms in the sum are irrelevant as being exponentially suppressed.

In (B.6), the term $\left(\frac{d}{dz} \frac{z}{e^z - 1} \right)_{z=z_n}$ can either be used for the quantity in W^+ or W^- , or even for the average of the two with increased precision. Fortunately, the two will prove to differ only in a subleading order, and we do not need to specify the choice. We proceed by rewriting Δz_n as

$$\Delta z_n = [\Delta\alpha + b(\Delta\tau^2 - 2\tau\Delta\tau)] - 2\Delta\tau\sqrt{b} y_n \tag{B.8}$$

(a form that is valid on both sides W^+ and W^-), with which we evaluate the sum (B.6) as

$$\begin{aligned}
& \underbrace{[\Delta\alpha + b(\Delta\tau^2 - 2\tau\Delta\tau)]}_{\text{both terms } \mathcal{O}(N^{-1})} \sum_{n=1}^{\infty} \left(\frac{d}{dz} \frac{z}{e^z - 1} \right)_{z=z_n} \\
& - 2\Delta\tau\sqrt{b} \sum_{n=1}^{\infty} \left(\frac{d}{dz} \frac{z}{e^z - 1} \right)_{z=z_n} \cdot y_n \\
& \approx \mathcal{O}(N^{-1}) \left[\mathcal{O}(b^0) + \underbrace{\frac{1}{\sqrt{b}} \int_{y_1}^{\infty} \left(\frac{d}{dz} \frac{z}{e^z - 1} \right)_{z=\alpha+y^2} dy}_{\mathcal{O}(b^0)} \right] \\
& - 2\Delta\tau\sqrt{b} \left[\mathcal{O}(b^0) + \frac{1}{\sqrt{b}} \int_{y_1}^{\infty} \left(\frac{d}{dz} \frac{z}{e^z - 1} \right)_{z=\alpha+y^2} \cdot \underbrace{y dy}_{\frac{1}{2} dz} \right]. \tag{B.9}
\end{aligned}$$

Among the obtained $2+2=4$ terms, the first three provide only an $\mathcal{O}(N^{-1/2})$ correction to the fourth term, which we calculate as

$$\begin{aligned}
-\Delta\tau \int_{z_1}^{\infty} \left(\frac{d}{dz} \frac{z}{e^z - 1} \right) dz &= \Delta\tau \frac{z_1}{e^{z_1} - 1} \\
&= \Delta\tau [1 + \underbrace{\mathcal{O}(\alpha + y_1^2)}_{\mathcal{O}(N^{-1})}] = -\frac{1}{2} + \mathcal{O}(N^{-1}). \tag{B.10}
\end{aligned}$$

Hence, we conclude that

$$b\Delta f + N\Delta\alpha \approx -\frac{1}{2} + \mathcal{O}(N^{-1/2}), \tag{B.11}$$

or

$$\frac{\Delta f}{N} \approx -\frac{1}{2} \frac{t}{N} - \Delta(t\alpha) + \mathcal{O}(N^{-1/2}), \tag{B.12}$$

which is (34).

References

- [1] M. Reed and B. Simon, Methods of Modern Mathematical Physics II, Fourier analysis, self-adjointness, Academic Press, New York, 1975.
- [2] N.I. Akhiezer and I.M. Glazman, Theory of Linear Operators in Hilbert Space, Vol.II, Pitman Advanced Publishing Program, Boston, 1981.
- [3] S. Albeverio, F. Gesztesy, R. Høegh-Krohn and H. Holden, Solvable Models in Quantum Mechanics, 2nd ed., Ams Chelsea Pub., 2004.

- [4] T. Cheon, T. Fülöp and I. Tsutsui, Ann. Phys. 294 (2001) 1.
- [5] I. Tsutsui, T. Fülöp and T. Cheon, J. Math. Phys. 42 (2001) 5687.
- [6] T. Fülöp and I. Tsutsui, Phys. Lett. A264 (2000) 366.
- [7] P. Exner and H. Grosse, Some properties of the one-dimensional generalized point interactions (a torso), eprint arXiv:math-ph/9910029.
- [8] T. Cheon, I. Tsutsui and T. Fülöp, Phys. Lett. A330 (2004) 338.
- [9] Quantum pressure on a Dirichlet boundary arising from a single energy level, rather than from the entire system of energy levels populated in a thermal distribution, has been discussed in
D. Berman, Am. J. Phys. 59 (1991) 937.
- [10] T. Fülöp, H. Miyazaki and I. Tsutsui, Mod. Phys. Lett. A 18 (2003) 2863.
- [11] I. Tsutsui and T. Fülöp, Int. Journ. Quant. Inf. 1 (2003) 543.
- [12] The allowed set of boundary conditions (1) forms the group $[U(1)]^4$ representing the possible self-adjoint domains of the free Hamiltonian in the interval $[-l, l]$ divided into two. If we allow the partition to transmit particles, then the boundary condition can be more general than (1) and given by $U(2) \times [U(1)]^2$ (see [1–3]).
- [13] A. Fuhrer, S. Lüsher, T. Ihn, T. Heinzel, K. Ensslin, W. Wegscheider and M. Bichler, Nature 413 (2001) 822.
- [14] J. McDougall and E.C. Stoner, Phil. Trans. A 237 (1939) 67.
- [15] I.S. Gradshteyn and I.M. Ryzhik (Ed.), Table of Integrals, Series, and Products, Academic Press, San Diego, 2000.
- [16] T. Fülöp, I. Tsutsui and T. Cheon, J. Phys. Soc. Jpn. 72 (2003) 2737.